Multiple Reggeon exchange from summing QCD Feynman diagrams

Y. J. Feng* and C. S. Lam†
Department of Physics, McGill University, 3600 University St., Montreal, P.Q., Canada H3A 2T8
(Received 17 June 1996)

Multiple Reggeon exchange supplies subleading logarithms that may be used to restore unitarity to the Low-Nussinov Pomeron, provided it can be proven that the sum of Feynman diagrams to all orders gives rise to such multiple Regge exchanges. This question cannot be easily tackled in the usual way except for very low-order diagrams, on account of delicate cancellations present in the sum which necessitate individual Feynman diagrams to be computed to subleading orders. Moreover, it is not clear that sums of high-order Feynman diagrams with complicated crisscrossing of lines can lead to factorization implied by the multi-Regge scenario. Both of these difficulties can be overcome by using the recently developed non-Abelian cut diagrams. We are then able to show that the sum of s-channel-ladder diagrams to all orders does lead to such multiple Reggeon exchanges. [S0556-2821(97)06007-4]

PACS number(s): 12.38.Cy

I. INTRODUCTION

The gluon in QCD Reggeizes in the leading-log approximation. The coupling constant (g) and the energy ($\sqrt{s}$) of sum of one-Reggeized-gluon (1RG) diagrams come in the form $g^2(g^2\ln s)^p$, where $g^2 \ll 1$, $g^2 \ln s \sim 1$, and p is a non-negative integer. The sum of 2RG diagrams are of the form $g^4(g^2\ln s)^p$, and more generally the mRG amplitude is given by sums of terms of the form $g^{2m}(g^2\ln s)^p$.

For quark-quark elastic scattering at high energy and fixed momentum transfer, the color exchanged in a 1RG amplitude is an octet, and that for a 2RG amplitude is either an octet or a singlet. The 2RG amplitude being a factor $g^2 \ll 1$ down from the 1RG amplitude, its octet contribution can be neglected, but its singlet part must be kept, for there is no competing contribution from the 1RG amplitude. This singlet part is just the Pomeron proposed by Low and Nussinov [1].

The leading-log Pomeron amplitude obtained this way [2,3] violates unitarity. It leads to a total cross section with a power growth in s, which is forbidden by the Froissart bound. To unitarize the Balitskii-Fadin-Kuraev-Lipatov (BFKL) equation [2] it is, therefore, necessary to include subleading-log contributions.

Subleading logarithms are notoriously difficult to extract from Feynman diagrams. This has been carried out in the two-loop approximation where the correction to the Reggeized gluon trajectory has been obtained [4]. However, it is almost certain that this cannot be carried out to all orders. Nevertheless, subleading-log contributions to the Pomeron do not necessarily require subleading logarithms from sums of Feynman diagrams. For example, leading-log calculation of Feynman diagrams contributing to 2RG exchanges gives subleading-log correction to the octet amplitude. Hence, there is a hope in unitarizing the Pomeron amplitude without having to invoke difficult subleading-log calculations. In fact, s-channel unitarity in all color channels is formally satisfied if all multiple RG exchanges are added in, as shown in the *Reggeized diagrams* in Fig. 1. To allow for shadows produced by inelastic scatterings, we must include production of gluons from the RG's in the intermediate states, though creation of quark pairs will be ignored in the present discussion. Whether this proposal of unitarization [3], without including subleading terms in individual sums of Feynman diagrams, is correct or not remains an open question which we simply cannot discuss until more is known.

The necessity of including multiple-RG exchange diagrams can be understood in a completely different way, totally within the framework of leading-log approximations. Imagine we are dealing with an SU(N_c) color theory in which quarks carry an arbitrary color. Then, there are many independent color amplitudes, more so if $N_c \gg 1$ and quarks carrying a large color. To retain the *leading-log* contribution of every one of these independent color amplitudes, we must retain the mRG contributions for every m. So, even staying within leading logarithms, those multiple-RG exchanges are required for a color SU(N_c) theory with arbitrary quark colors. For that reason we shall carry out our calculations below

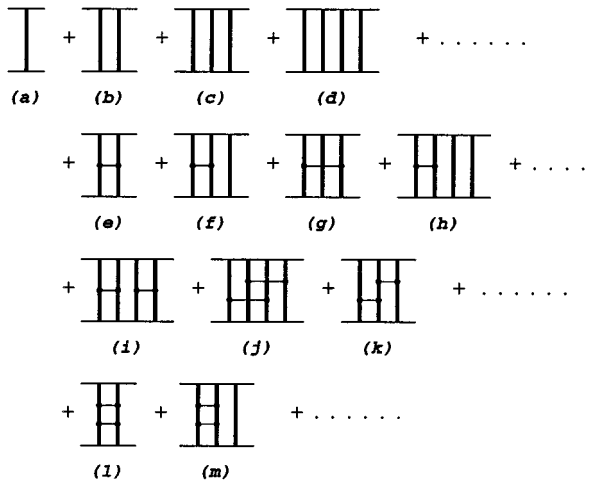

FIG. 1. Multi-Reggeon exchange diagrams.

*Electronic address: feng@physics.mcgill.ca
†Electronic address: lam@physics.mcgill.ca

for an arbitrary N_c and every quark color. Since spin is unimportant in high energy scattering [2,3], this has the added advantage that whatever we obtain is automatically valid for gluon-gluon scattering as well.

What is missing in this scheme is the proof that the *Reggeized factorization hypothesis* is indeed correct, that the sum of Feynman diagrams in the leading-log approximation does factorize into sums of these multiple-RG amplitudes.

To be sure, the hypothesis has been verified explicitly up to the sixth order, and partially up to the eighth and tenth orders [2,5,6], but because of the presence of delicate cancellations, it is difficult to carry similar calculations to higher orders. In fact, these delicate cancellations have not been completely verified even in the eighth and the tenth orders.

The problem is the following. In Feynman gauge calculation, which we shall adopt throughout, the leading-log contributions in some color amplitudes get canceled out when several Feynman diagrams are summed [5–7]. Consequently, to compute the *sum* of diagrams to leading-log accuracy, we need to calculate individual diagrams to subleading-log precision. Occasionally, this can be accomplished without much pain by using $s\leftrightarrow u$ symmetry, but more often not. To the extent that subleading logarithms are very difficult to compute, calculations to higher-order diagrams do appear to be quite forbidding.

Even if we manage to overcome this hurdle, the verification of Reggeized *factorization* from sums of Feynman diagrams, with lines crossing one another in very complicated ways, would still seem to be extremely difficult.

Fortunately, there is a chance to overcome both of these difficulties by using *non-Abelian cut diagrams* [7] in place of the usual Feynman diagrams. Non-Abelian cut diagrams are resummations of Feynman diagrams with these delicate cancellations removed, so that each of them can be computed just in the leading-log approximation. Moreover, factorization is natural to the non-Abelian cut diagrams, because they are the graphical manifestation of a ''multiple commutator formula,'' which in turn was derived from a ''factorization formula'' [8], and it is this same factorization formula that will be used to demonstrate Reggeized *factorization* hypothesis for a class of diagrams.

Non-Abelian cut diagrams will be reviewed in the next section. Some of their properties, including the assertion of the absence of delicate cancellations in these cut diagrams but their presence in usual Feynman diagrams, will be discussed in Sec. III. In this paper we shall study in detail, and be able to prove, the Reggeized factorization hypothesis for a particular simple class of diagrams, the s-channel-ladder diagrams. It is this class of diagrams in QED that can be summed up into an explicit eikonal form, so one would expect it to be the simplest set to study in QCD as well for multiple-RG exchanges and unitarization. However, with color complication, the QCD case is much harder to deal with than the QED case, the details of which are discussed in Sec. IV. For more complicated non-Abelian cut diagrams in QCD, we are not yet able to prove the Reggeized factorization, but the success for the s-channel-ladder diagrams is encouraging. Finally, a short summary and outlook are provided in Sec. V.

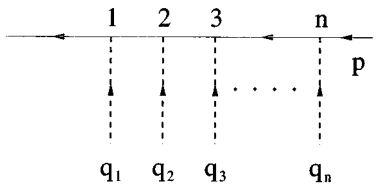

FIG. 2. A tree diagram with n bosons emitted or absorbed.

II. NON-ABELIAN CUT DIAGRAMS

Non-Abelian cut diagrams [7] represent a resummation of Feynman diagrams. They are not the same as Cutkosky cut diagrams which compute discontinuities of single Feynman diagrams.

A non-Abelian cut diagram differs from a Feynman diagram in having certain ''high speed'' propagators cut. The cut lines occur among those carrying a large momentum p, with comparatively small amount of momenta q_i transferred away at each interaction vertex. In that case, the approximation

$$\left(p+\sum_{j=1}^{i} q_j\right)^2 - m^2 \simeq 2p\cdot\sum_{j=1}^{i} q_j \equiv \sum_{j=1}^{i} \omega_j \tag{2.1}$$

is valid, so the denominators of the Feynman propagators for these lines are simplified to $(\Sigma_{j=1}{}^{i}\omega_j + i\epsilon)^{-1}$.

Within this approximation, the QCD tree diagram for a propagating quark shown in Fig. 2 is

$$-2\pi i\,\delta\left(\sum_{j=1}^{n}\omega_j\right)\left(\prod_{i=1}^{n-1}\frac{1}{\Sigma_{j=1}^{i}\omega_j+i\epsilon}\right)\cdot t_1 t_2\cdots t_n\cdot V$$
$$\equiv a[12\cdots n]\cdot t[12\cdots n]\cdot V\ , \tag{2.2}$$

where t_i are the color matrices of the quark, and $t[12\cdots n]\equiv t_1 t_2\cdots t_n$. The numerator with the normalization convention $\bar{u}u=1$ can be approximated by

$$V=\frac{1}{2M}\prod_{i=1}^{n}(2p^{\mu_i})\ , \tag{2.3}$$

where μ_i are the Lorentz indices of the gluons and M is the quark mass.

The tree diagram in Fig. 2 will be denoted by $[12\cdots n]$, according to the order of the gluons. If the gluons are labeled differently, say as $[\sigma_1\sigma_2\cdots\sigma_n]$, then the corresponding spacetime amplitude and color factor will be similarly designated as $a[\sigma_1\sigma_2\cdots\sigma_n]$ and $t[\sigma_1\sigma_2\cdots\sigma_n]$.

Before discussing the non-Abelian cut diagrams it is necessary to introduce some notation. If $[T_i]$ are tree diagrams, then $[T_1T_2\cdots T_A]$ represents the tree diagram obtained by merging these A trees. For example, if $[T_1]=[123]$ and $[T_2]=[45]$, then $[T_1T_2]=[12345]$. The notation $\{T_1;T_2;\cdots;T_A\}$, on the other hand, is used to denote the *set* of all tree diagrams obtained by *interleaving* the trees $T_1,T_2,\ldots,T_A$ in all possible ways. This set contains $(\Sigma_a n_a)!/\Pi_a n_a!$ trees if n_a is the number of gluon lines in the tree T_a. In the example above, $\{T_1;T_2\}$ contains the following $5!/3!2!=10$ trees: [12345], [12435], [12453], [14235], [14253], [14523], [41235], [41253], [41523], and [45123].

Correspondingly, $a\{T_1;T_2;\cdots;T_A\}$ will represent the sum of the amplitudes $a[T]$ for every tree T in this set.

The non-Abelian cut diagram [7] is derived from the *multiple commutator formula* [8], which states that

$$\sum_{\sigma\in S_n} a[\sigma]t[\sigma]=\sum_{\sigma\in S_n} a[\sigma]_c t[\sigma]'_c \ . \tag{2.4}$$

This is a resummation formula for the non-Abelian tree amplitude (2.2), summed over all $n!$ permutations $[\sigma]\equiv[\sigma_1\sigma_2\cdots\sigma_n]$ of $[12\cdots n]$. The spacetime part of the *cut amplitude* $a[\sigma]_c$ is obtained from the *cut diagram* $[\sigma]_c$, and the color factor $t[\sigma]'_c$ is obtained from the *complementary cut diagram* $[\sigma]'_c$. All of these will be explained below.

The multiple commutator formula in turn was derived from the *factorization formula* [8], which states that

$$a\{T_1;T_2;\cdots;T_A\}=\prod_{a=1}^{A} a[T_a] \ . \tag{2.5}$$

This is a sum rule expressing factorization of sums of certain tree amplitudes. It is this same formula that proves to be invaluable in showing the Reggeized *factorization* later.

A special case of the factorization formula is well known. If $n_a=1$ for every a so that the tree $[T_a]=[a]$ is simply a vertex, then $\{1;2;\cdots;A\}$ is the set of $A!$ permutation of the tree $[12\cdots A]$, and the factorization formula is just the well-known *eikonal formula* [9].

We shall now proceed to define the cut diagrams and the cut amplitudes. To each Feynman tree diagram $[\sigma]=[\sigma_1\sigma_2\cdots\sigma_n]$ of the type shown in Fig. 2, we associate with it a *cut diagram* $[\sigma]_c$ by putting cuts on specific fermion propagators as follows. Proceed from left to right, put a cut after a gluon if and only if a smaller number does not occur to its right. Continuing thus until reaching the end of the tree, and we get the cut diagram. An external line would be considered equivalent to a cut so there is never an explicit cut put in at the end of the tree.

The written notation for a cut will be a vertical bar behind a gluon. Using that notation, here are some illustrations of where cuts are put into Feynman trees: $[1234]c=[1|2|3|4]$, $[3241]c=[3241]$, *and* $[2134]_c=[21|3|4]$.

The *complementary cut diagram* $[\sigma]'_c$ is one where lines cut in $[\sigma]_c$ are not cut in $[\sigma]'_c$, and vice versa. Thus $[1234]'_c=[1234]$, $[3241]'_c=[3|2|4|1]$, and $[2134]'_c=[2|134]$.

The spacetime part of the cut amplitude $a[\sigma]_c$ is simply the Feynman amplitude $a[\sigma]$ with the cut propagator taken to be $-2\pi i\delta(\Sigma_j\omega_j)$ instead of the usual $(\Sigma_j\omega_j+i\epsilon)^{-1}$. In this way, it is the same cut propagator as in the Cutkosky cut diagram, but here cuts are placed only on high speed fermion lines, and as Eq. (2.4) indicates, the non-Abelian cut diagrams represent a resummation and not a discontinuity.

The color factor $t[\sigma]'_c$ is determined from the complementary cut diagram $[\sigma]'_c$. It is obtained from $t[\sigma]$ by replacing the product of color matrices separated by cuts with their commutators. For example, $t[1234]'_c=t[1234]=t_1t_2t_3t_4$, $t[3214]'_c=t[3|2|4|1]=[t_3,[t_2,[t_4,t_1]]]$, and $t[2134]'_c=t[2|134]=[t_2,t_1]t_3t_4$.

A Feynman diagram for quark-quark scattering can be obtained by connecting two trees like Fig. 2 together via the gluon lines, perhaps with the help of triple-gluon and four-gluon vertices and other propagators in between. Since Eq. (2.4) is valid for off-shell gluons, it can be applied to one of the two quark trees carrying large momentum even though it is tied up in a loop diagram. Unless otherwise stated, relation (2.4) will always be applied to the upper quark tree, so cuts are normally made only on this line. The rest of the propagators remain uncut and the diagram is otherwise the same as an ordinary Feynman diagram.

III. ABSENCE OF DELICATE CANCELLATIONS

We mentioned in the Introduction that complete cancellation of the leading-log contributions to individual Feynman diagrams may occur in their sum. When this occurs computations become extremely difficult as subleading contributions must then be included to get a finite sum. We shall show in this section that this will never happen in the sum of *non-Abelian cut diagrams*, that the high energy behavior of the individual diagrams is the same as their sum, at least when the Reggeized factorization hypothesis is correct. This is why it is so much more advantageous to investigate Regge behavior with non-Abelian cut diagrams than with Feynman diagrams.

The color factor of a Feynman diagram [3,5] or a non-Abelian cut diagram [7] will be decomposed into sums of color factors of planar diagrams using the commutation relation

$$[t_a,t_b]=if_{abc}t_c \ , \tag{3.1}$$

as well as the sum rules

$$f_{abc}f_{abd}=2c\,\delta_{cd} \ , \quad i^3f_{adg}f_{bed}f_{cge}=cif_{abc} \ , \tag{3.2}$$

where $c=N_c/2$ for a color SU(N_c) group, and t_a is the color matrix of the quark in any representation. In particular, if it is in the adjoint representation, then $(t_a)_{bc}=if_{bac}$, and this is represented graphically by a triple-gluon vertex read in a clockwise order. These relations are shown in Fig. 3 where a cut represents a commutator. Using these figures, decomposition into planar diagrams can be accomplished in a graphical way. For details and concrete illustrations, see Refs. [5] and [7].

The resulting planar color factors appearing in the Regge diagrams of Fig. 1 will be called the *Regge color factors*. If the Reggeized factorization hypothesis is correct, only Regge color factors will survive when all the diagrams are summed.

Color factors for the non-Abelian cut diagrams are computed from their complementary cut diagrams, and those with $m-1$ *uncut* propagators on the upper quark line contain Regge color factors with *at most* mRG exchanges. This statement is a simple consequence of the graphical construction procedure for the Regge color factors [7]. See Appendix A.

The corresponding cut diagram for the spacetime amplitude has $m-1$ cut lines. Now, each loop in a spacetime diagram can contribute at most one ln$s$ factor, but this factor will be absent in any loop containing a cut propagator. This is so because the Feynman propagator giving rise to the ln$s$ factor through integration is now replaced by a δ function

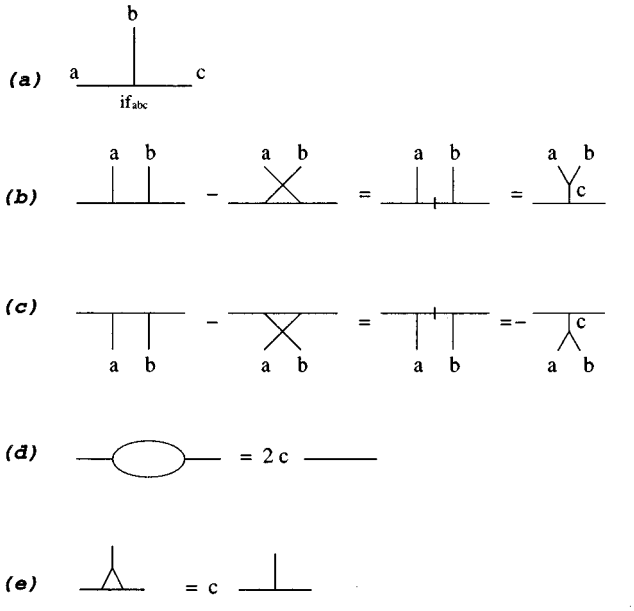

FIG. 3. Color matrices and their relations (3.1) and (3.2) in graphical forms.

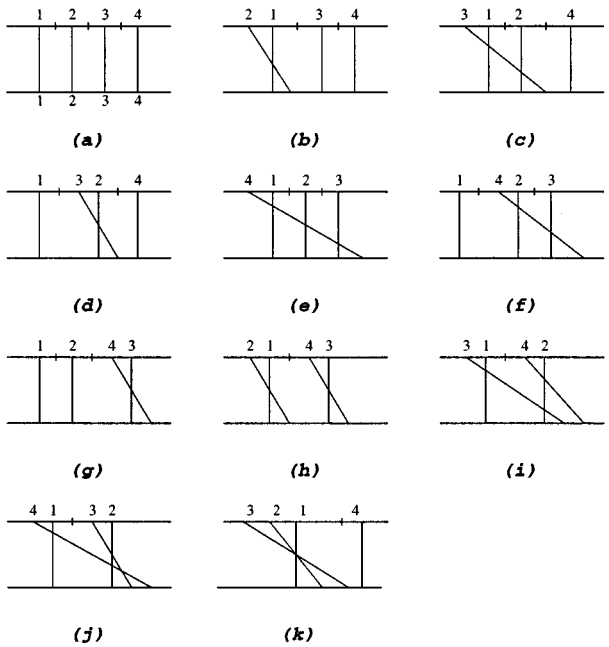

FIG. 4. Examples of eighth order s-channel-ladder cut diagrams.

[5,7]. With $m-1$ cut propagators, $m-1$ potential ln$s$ factors are lost, so the spacetime amplitude can grow at most like $g^{2m}(g^2\ln s)^p$.

Thus a non-Abelian cut diagram with an mRG Regge color factor increases with energy at most like $g^{2m}(g^2\ln s)^p$. If the Reggeized factorization hypothesis is correct, this is also the energy behavior of the sum of all non-Abelian diagrams with this same Regge color factor. Hence no cancellation of leading logarithms occurs in the sum of non-Abelian cut diagrams.

This also means that in the leading-log approximation, there is no need to include in a complementary cut diagram with $m-1$ uncut lines those Regge color factors with less than mRG exchanges.

From these discussions we can also see why delicate cancellations are generally expected for Feynman diagrams if the Reggeization hypothesis is valid. A Feynman diagram has no cut in its spacetime diagram, nor in its color factor. The former tends to give rise to more ln$s$ factors than a corresponding cut diagram, and the latter will generally yield Regge color factors with larger m. For both reasons there are too many ln$s$ powers compared to the Reggeized behavior of $g^{2m}(g^2\ln s)^p$, so delicate cancellations eliminating these powers must take place.

IV. s-CHANNEL-LADDER CUT DIAGRAMS

A. Description of the diagrams

s-channel-ladder diagrams are obtained by joining together the gluons of two quark trees like Fig. 2. If we number the gluons attached to the lower quark tree in the order $[123\cdots n]$, then the order of gluons along the upper quark tree can be used to specify the s-channel-ladder diagram. Cut diagrams are determined by the rules discussed in Sec. II, and cut propagators on the upper quark tree will be indicated by a vertical bar as before. In this notation, Figs. 4(a)–4(k) are, respectively, $[1|2|3|4]$, $[21|3|4]$, $[31|2|4]$, $[1|32|4]$, $[41|2|3]$, $[1|42|3]$, $[1|2|43]$, $[21|43]$, $[31|42]$, $[41|32]$, and $[321|4]$. Unless otherwise stated, propagators along the lower quark tree will remain uncut, so when we refer to cut and uncut propagators, we will usually be speaking of those along the upper quark tree.

We will use the abbreviation SC to denote *s-channel-ladder cut diagram*, and the notation SCC to denote *s-channel-ladder complementary cut diagram*. The former is used to compute spacetime amplitudes, and the latter to compute color factors. Cut propagators in SC become uncut propagators in SCC and vice versa.

From the rules of Sec. II, we conclude that all propagators of the planar SC diagram are to be cut, giving rise to $[1|2|\cdots|n]$, as illustrated in Fig. 4(a). For other SC diagrams, cuts are placed behind a number if and only if there is not a smaller number to its right.

We can phrase this in a way independent of the numberings of the gluon lines. All SC diagrams are obtained from the planar diagram by pulling the upper ends of some gluon lines leftward. Once a gluon line is moved, the cut to its right disappears. Thus, cuts appear to the right of all vertical (v) lines but do not appear to the right of any slanted (s) line.

According to the discussions in Sec. III, in the leading-log approximation, we need to retain only the mRG Regge color factors from a SCC diagram with $m-1$ uncut propagators, and only the SC diagrams with $m-1$ cuts on the upper tree whose ln$s$ power is given by $g^{2m}(g^2\ln s)^p$, and not lower. It is shown in Appendix B that these *saturated* SC diagrams are those without adjacent uncut propagators on the upper tree. For example, Figs. 4(a)–4(j) are saturated, and should be retained, but Fig. 4(k) is not, and can be discarded.

Accordingly, along the *upper quark line*, the line to the right of an s line is always a v line, and not another s line because diagrams of the latter kind will not contribute to the leading logarithm. We shall refer to the v line to the right of

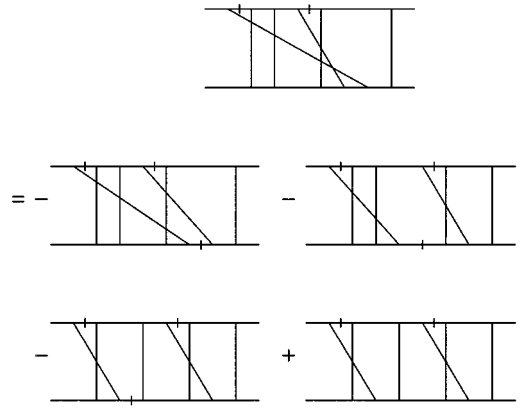

FIG. 5. An example of the decomposition of SCC diagrams into sums of reduced diagrams.

an s line as its *associated vertical line*, and this pair of s,v lines as a *skeleton cross*.

B. Color factors and reduced diagrams

Given a saturated SCC diagram, we need to decompose its color factor into combinations of Regge color factors. This is accomplished by using Fig. 3 to pull the *lower end* of every s line leftward, until it sits just to the right of its associated v line, a position to be referred to as its *home position*. Figure 5 gives an illustration of how this is done for one s line; the same should be carried out with the other s line as well. As a result, the SCC diagram is given by a sum of many *reduced diagrams*. A reduced diagram is distinguished by having cuts along the *lower tree* to the right of every s line, except when it occurs in its home position, as illustrated by the last diagram of Fig. 5, in which case a cut is not necessary.

For later discussions it would be convenient to have an analytical notation for the reduced diagrams. We shall use v_i,s_i to denote the ith pair of skeleton lines, and m_a to denote the rest of the vertical lines. Then, a reduced diagram can be labeled by the cut tree along its bottom line. For example, the four diagrams in Fig. 6 can be labeled, respectively, as $[m]$, $[vs]$, $[vs|m]$, and $[v_1s_1|v_2s_2|m]$.

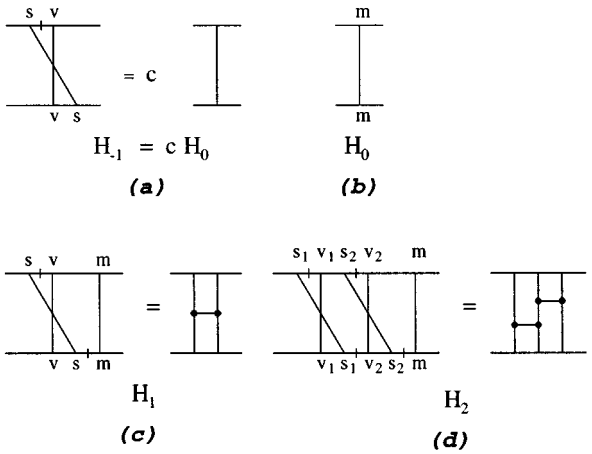

FIG. 6. Examples of how primitive color factors are obtained from reduced diagrams.

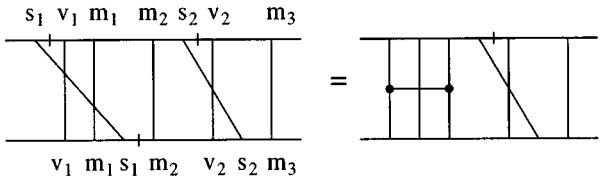

FIG. 7. An example of a disconnected reduced diagram and the corresponding Regge color factor.

The color factors for reduced diagrams can be rendered planar using the rules of Fig. 3. See Fig. 6 for examples. The resulting color factor of a reduced diagram may or may not be *connected* after the upper and lower quark lines are removed. For example, those in Fig. 6 are connected and the one in Fig. 7 is not. It turns out that the only connected Regge color factors encountered in the reduction of SCC diagrams are those shown in Fig. 6, and those similar to Fig. 6(d) but with $p>2$ slanted lines. By using Fig. 3 these can be turned into p horizontal lines, with the one to the right always lying at a higher level than the one to its left. These connected Regge color factors will be denoted as H_p, with $p=-1,0,1,2,\ldots$ (see Fig. 6). Except for $H_{-1}=cH_0$, they are all independent.

Potentially, there may also be those like Figs. 8 and 9, but as shown in the figures and more generally in Appendix A, they all turn out to be zero in the leading-log approximation.

It is also shown in Appendix A that in the leading-log approximation, the color factor of a disconnected reduced diagram is given just by the product of the color factors of its connected components, and it is this special property that allows Reggeized factorization to take place. Thus, the most general color factor encountered in SCC diagrams is of the form $\Phi=\Pi_{p=-1}^{\infty}(-)^{pf_p}(H_p)^{f_p}$.

We shall use $[H_p]$ to denote the reduced diagram giving rise to the connected Regge color factor H_p. In cut-tree notations, these are

$$[H_{-1}]=[vs], \tag{4.1}$$

$$[H_0]=[m],$$

$$[H_1]=[vs|m],$$

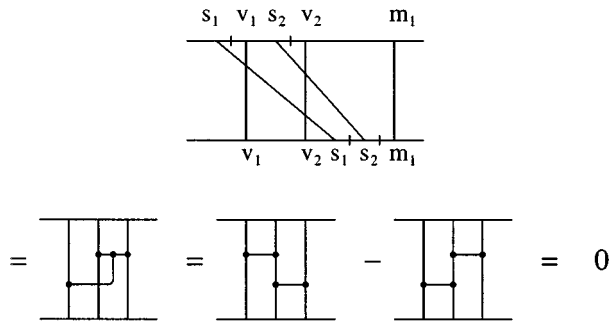

FIG. 8. An example of a connected reduced diagram that is not primitive.

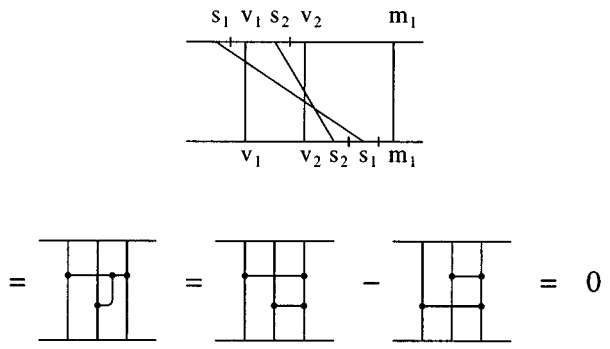

FIG. 9. Another example of a connected reduced diagram that is not primitive.

$$[H_2]=[v_1s_1|v_2s_2|m],$$

$$[H_p]=[v_1s_1|v_2s_2|\cdots v_ps_p|m]\ ,\quad (p\geqslant 1).$$

For a general Φ, there would be many reduced diagrams giving rise to the same Regge color factor. They differ from one another in having the f_p copies of $[H_p]$ for different p's merged in different ways. We shall denote this set of reduced diagrams for a given color factor Φ by

$$\{\Phi\}=\left\{\prod_p\ (-)^{pf_p}(H_p)^{f_p}\right\}_{\text{distinct}}$$
$$=\{[H_{-1}];\cdots;[H_0];\cdots;[H_1];\cdots;[H_2];\cdots;\cdots\}$$
$$\times\prod_p\ (-)^{pf_p}/f_p!\ , \tag{4.2}$$

where the ellipses after each $[H_p]$ is an instruction to repeat the same $[H_p]$ f_p times, separated by semicolons. The sign $(-)^p$ associated with H_p comes about because of the minus sign associated with each cut. The notation in Eq. (4.2) for interleaving the cut trees is similar to the notation $\{T_1;T_2;\cdots\}$ explained in Sec. II for interleaving uncut trees T_i, but with two differences. First, lines separated by cuts are to be thought of as being fused together by the cut, so lines from other cut trees can never be inserted between them. Second, each cut diagram in $\{[H_p];\cdots\}$ is going to occur $f_p!$ times because of the identical nature of those diagrams. We allow only distinct diagrams in $\{\Phi\}$ so the division by $\Pi_p f_p!$ in Eq. (4.2) is a formal way of removing such redundancies.

Given a reduced diagram in $\{\Phi\}$, there are many different SCC that can give rise to it. We shall denote the set of all SCC diagrams that can give rise to a reduced diagram in $\{\Phi\}$ by $\{\Phi\}_S$. These SCC diagrams can be obtained from the cut trees in $\{\Phi\}$ by getting rid of their cuts by moving the s-lines rightward in all possible ways. Instead of first interleaving the cut trees $[H_p]$ and then getting rid of the cuts, $\{\Phi\}_S$ can also be obtained by reversing the two operations, by first getting rid of the cuts and then interleaving the uncut trees, in the following way.

Start from an $[H_p]$, get rid of the cuts by moving the s-lines rightward, to construct all SCC diagrams h_p^i $(i=1,2,\ldots)$ that reduce to $[H_p]$. In cases such as Figs. 6(a)–6(c) where there is only one tree for each $[H_p]$, the degeneracy index $i=1$ will be omitted. This index is, however, needed in other cases. For example, $[H_2]=[v_1s_1|v_2s_2|m]$ in Fig. 6(d) gives rise to the uncut trees $h_2^1=[v_1v_2s_1ms_2]$, $h_2^2=[v_1v_2ms_1s_2]$, and $h_2^3=[v_1v_2ms_2s_1]$. The set of all h_p^i for a fixed p will be denoted by $\{H_p\}_S$.

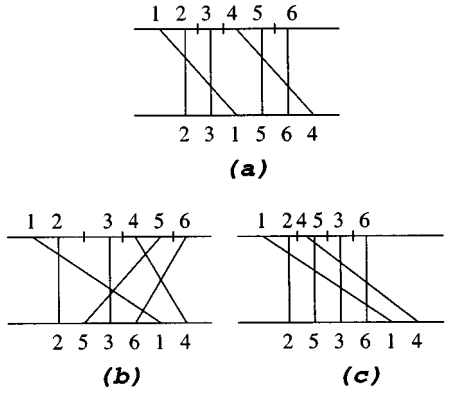

FIG. 10. Two SC diagrams in the set {231;564}. Diagram (b) is identical to diagram (c).

The set of *distinct* SC or SCC diagrams obtained by interleaving f_p trees in $\{H_p\}_S$ together is just $\{\Phi\}_S$.

C. Factorization of sums of spacetime amplitudes

We proceed to compute the sum of those spacetime amplitudes of all saturated SC diagrams with a common Regge color factor $\Phi=\Pi_p((-)^pH_p)^{f_p}$. The relevant spacetime diagrams to be summed are those in the set $\{\Phi\}_S$.

Using the factorization formula (2.5) on the *lower* tree, one gets

$$a\{\Phi\}_S=\sum_{[T]\in\{\Phi\}_S}a[T]=\prod_p\ \frac{1}{f_p!}(a\{H_p\}_S)^{f_p}\ , \tag{4.3}$$

where

$$\frac{1}{f_p!}(a\{H_p\}_S)^{f_p}\equiv\sum\ \frac{1}{m_i!}(a[h_p^i])^{m_i}\ , \tag{4.4}$$

with the sum taken over all $m_i\geqslant 0$ subject to $\Sigma_i m_i=f_p$. Thus, $a\{H_p\}_S=\Sigma_i a[h_p^i]$. The factorials in the denominators of Eq. (4.4) arise because of the necessity to keep only distinct diagrams in $\{\Phi\}_S$.

The factorizations (4.3) and (4.4) for the lower tree can be extended to a factorization for the SC amplitudes. To do so we need to use explicitly the cut property of the *upper* tree, that the only uncut propagators are those inside the skeleton crosses. To illustrate this point let us look at Fig. 10. Both the (lower) tree [231564] in Fig. 10(a) and the tree [253614] in Fig. 10(b) belong to the set {231;564}, but if we keep the upper ends of the gluon lines fixed in Figs. 10(a) and 10(b), permuting the lower ends of the lines to get from Figs. 10(a) to 10(b) does *not* change the SC diagram, Fig. 10(a), back to another SC diagram. Figure 10(b), with lines 5 and 6 slanting the wrong way, cannot be an SC diagram. However, by making explicit use of the commuting properties of the amplitude

for the *upper tree*, $a[12|3|45|6]=a[12]a[3]a[45]a[6]=a[12|45|3|6]$, Fig. 10(b) can be redrawn as Fig. 10(c), which is an SC diagram. This can always be done so factorization of the lower tree does lead to a factorization of the sum of saturated SC amplitudes.

An SC diagram contains the lower tree, but it also contains gluon propagators, quark propagators along the upper tree, vertex factors, and loop integrations. In light-cone coordinates, $q_\pm=q^0\pm q^3$, the measure of loop integration is

$$\frac{d^4q}{(2\pi)^4}=\frac{d^2q_\perp}{(2\pi)^2}\frac{dq_+dq_-}{8\pi^2} \quad . \tag{4.5}$$

If the Dirac spinors are normalized to $\overline{uu}=1$, and a common factor is taken out of the T-matrix amplitude $\mathcal{T}=-(s/2M^2)\mathcal{A}$, then each factorized amplitude $a\{H_p\}_S=\Sigma_i a[h_p^i]$ corresponds to a saturated SC amplitude $\mathcal{A}\{H_p\}_S(\Delta)=\Sigma_i\mathcal{A}[h_p^i](\Delta)$, where we have indicated explicitly the dependence on the momentum transfer Δ. The product of two lower-tree amplitudes $a\{H_a\}a\{H_b\}$ is turned into convolutions of two SC amplitudes:

$$[\mathcal{A}\{H_a\}_S*\mathcal{A}\{H_b\}_S](\Delta)\equiv(-i)\int\frac{d^2q_\perp}{(2\pi)^2}[\mathcal{A}\{H_a\}](\Delta-q_\perp)\times[\mathcal{A}\{H_b\}](q_\perp) \quad . \tag{4.6}$$

In obtaining Eq. (4.6), the identity

$$i\int\frac{dq_+dq_-}{8\pi^2}(-2\pi i)^2\delta(\sqrt{s}q_+)\delta(\sqrt{s}q_-)(2s)=-i \tag{4.7}$$

has been used.

The sum of all saturated SC amplitudes with the Regge color factor Φ is then given by

$$[\mathcal{A}\{\Phi\}_S](\Delta)=\prod_p\frac{1}{f_p!}[\mathcal{A}\{H_p\}_S]^{*f_p}(\Delta) \quad . \tag{4.8}$$

All the products in Eq. (4.8) are meant to be convolutions. In particular, $[\mathcal{A}\{H_p\}_S]^{*f_p}$ is taken to mean f_p convolutions of the same amplitude. In impact-parameter space, such convolutions are replaced by simple products.

D. $O(g^6)$ results

Let us now compare the general result of Eq. (4.8) with the $O(g^6)$ result of Ref. [7]. Except for the second-order tree diagram, they are shown in Fig. 7 of Ref. [7] as $B1_c$, $B2_c$, and $C15_c$ to $C20_c$. The spacetime amplitudes are given in Eq. (6.1) of that reference and were expressed in terms of $\mathcal{M}=-\mathcal{A}/g^2$; hence,

$$\mathcal{A}(\mathbf{G_1})=K_1-\ln s\frac{c}{2\pi}K_2, \tag{4.9}$$

$$\mathcal{A}(\mathbf{G_2})=-\frac{1}{2}iK_2+i\ln s\frac{c}{2\pi}K_3,$$

$$\mathcal{A}(\mathbf{G_3})=-i\ln s\frac{1}{2\pi}K_3,$$

$$\mathcal{A}(\mathbf{G_4})=-\frac{1}{6}K_3,$$

where the color factors $\mathbf{G_1}$, $\mathbf{G_2}$, $\mathbf{G_4}$, $\mathbf{G_3}$ are the color factors H_0, H_0^2, H_0^3, H_1 in the present paper, and where

$$K_n(\Delta)=i^{n-1}(*K_1)^n, \quad K_1(\Delta)=\frac{g^2}{\Delta^2} \quad . \tag{4.10}$$

The transverse functions K_n are related to the ones used in Ref. [7] by $K_n=g^{2n}I_n$.

The general result for $O(g^6)$ according to Eq. (4.8) is

$$[\mathcal{A}\{(-H_1)^a(H_0)^b\}_S](\Delta)=\frac{1}{a!b!}[\mathcal{A}\{H_1\}_S]^{*a}*[c\mathcal{A}\{H_{-1}\}_S+\mathcal{A}\{H_0\}_S]^{*b}(\Delta) \quad . \tag{4.11}$$

Substituting into Eq. (4.11) the explicit result obtained from Eq. (6.1) of Ref. [7],

$$\mathcal{A}\{H_0\}_S=\frac{g^2}{\Delta^2}=K_1,$$

$$\mathcal{A}\{H_{-1}\}_S=-\frac{g^2}{c\mathbf{G_1}}(B2_c)=-\ln s\frac{1}{2\pi}K_2,$$

$$\mathcal{A}\{H_1\}_S=-g^2/(c\mathbf{G_2}-\mathbf{G_3})(C20_c)=\ln s\frac{i}{2\pi}K_3, \tag{4.12}$$

we get

$$[\mathcal{A}\{(-H_1)^a(H_0)^b\}_S](\Delta)=\frac{1}{a!b!}\left[\ln s\frac{i}{2\pi}K_3\right]^{*a}*\left[K_1-\ln s\frac{c}{2\pi}K_2\right]^{*b}(\Delta). \tag{4.13}$$

The color factors $\mathbf{G_1}$, $\mathbf{G_2}$, $\mathbf{G_4}$ correspond to $(a,b)=(0,1),(0,2),(0,3)$, and the color factor $\mathbf{G_3}$ corresponds to $(a,b)=(1,0)$ but with an extra minus sign. Expanding Eq. (4.13), keeping only leading-log contributions and only up to $O(g^6)$, the result is the same as Eq. (4.9).

In particular, $O(g^6)$ diagrams receive only contribution from K_3 of Eq. (4.9), so that the total amplitude at leading logarithm is given by

$$\mathcal{M}=-is\ln s\frac{1}{4\pi M^2}K_3[c\mathbf{G_2}-\mathbf{G_3}] \quad . \tag{4.14}$$

This result can be compared with the one contained in Eqs. (56) and (68) of the JETP, Vol. **44**, paper cited in Ref. [2], where the color group is SU(2). According to these equations, the symmetric part of the amplitude is equal to

$$\mathcal{M}=-\frac{1}{4\pi^2M^2}[A^{(0)}\Gamma_{AA'}\Gamma_{BB'}+A^{(2)}\Gamma^{ij}_{AA'}\Gamma^{ij}_{BB'}]$$

$$=-is\ln s\frac{1}{4\pi M^2}\beta_3[\Gamma_{AA'}\Gamma_{BB'}-2\Gamma^{ij}_{AA'}\Gamma^{ij}_{BB'}], \tag{4.15}$$

where the Γ tensors are given in their Eqs. (14) and (15), and A,B and A',B' are, respectively, the initial and the final

isospin components of the external gluons. In the present case, $c=1$, and the symmetric part of the color factor appearing in our Eq. (4.14) can be computed to be

$$\mathbf{G_2}-\mathbf{G_3}=\delta_{AB}\delta_{A'B'}+\delta_{AB'}\delta_{A'B}-2\,\delta_{AA'}\delta_{BB'} \quad . \tag{4.16}$$

When this is substituted back into Eq. (4.14), the result agrees with Eq. (4.15) when the explicit expressions for the Γ tensors are used, and when we notice that their β_3 is the same as our K_3.

E. Reggeized factorization

The expression $\mathcal{A}\{H_0\}_S+c\,\mathcal{A}\{H_{-1}\}_S=K_1-(c/2\pi)\ln s K_2$ in Eqs. (4.11) and (4.13) is the first two terms of the Reggeized-gluon propagator

$$R_1(\Delta,s)=\frac{g^2}{\Delta^2}\exp[-\overline{\alpha(}\Delta)\ln s] \quad ,$$

$$\overline{\alpha(}\Delta)=\frac{c}{2\pi g^2}\Delta^2 K_2(\Delta) \quad . \tag{4.17}$$

The other terms come from t-channel-ladder and associated diagrams [2,3,5] not considered here. The term $\mathcal{A}\{H_1\}_S$ in Eq. (4.11) is one of the many terms contributing to the emission and reabsorption of an ordinary gluon from a Reggeized gluon, as indicated by the pattern H. Even to $O(g^6)$, it receives contributions from other diagrams as well [7]. When all these are taken into account, it is known that such emission and absorption can be constructed from the Lipatov vertex [2].

So, the factorized results (4.8) and (4.11) are the beginning of contributions that lead to *Reggeized* factorization, but the Reggeization property cannot be seen fully without including other diagrams. However, the Reggeized nature of the color factors does seem to emerge rather naturally.

V. SUMMARY AND OUTLOOK

In this paper we initiated a leading-log investigation on sums of Feynman diagrams contributing to multiple Reggeized-gluon exchanges. These diagrams are important because they supply non-leading-log contributions to the SU(3) gluon and Pomeron amplitudes, thereby restoring unitarity. In any case, they supply the leading contributions in an SU(N_c) color theory in which the colliding beams carry large color so they must be taken into account.

The central question studied in this paper is whether sums of Feynman diagrams in the leading-log approximation will factorize into multiple-Reggeon-exchange diagrams as depicted in Fig. 1. This ''Reggeized factorization hypothesis'' is nontrivial to prove for at least two reasons. First, it is known that there are delicate cancellations in sums of Feynman diagrams, so individual diagrams must be computed to subleading-log accuracy to ensure a finite contribution to the sum. This is a very difficult task for high order diagrams. Second, high order Feynman diagrams are very complicated, with lines crisscrossing in a complex pattern, so it is far from obvious that they will sum up and factorize into neat patterns as those displayed in Fig. 1. To date, factorization had been proved completely only to the sixth order, and partially to the eighth and tenth orders, by explicit calculations.

We prove in this paper the Reggeized factorization hypothesis for s-channel-ladder diagrams of any complexity. Both of the difficulties mentioned above are solved by using instead the technique of non-Abelian cut diagrams discussed in previous publications [7,8]. These cut diagrams are resummations of Feynman diagrams and are different from the Cutkosky cut diagrams.

For other diagrams the validity of the Reggeized factorization hypothesis is still under investigation.

ACKNOWLEDGMENTS

We thank Jean-René Cudell and Omid Hamidi-Ravari for interesting discussions. This research was supported in part by the Natural Science and Engineering Research Council of Canada, and the Fonds pour la Formation de Chercheurs et l'Aide à la Recherche of Québec, and Y.J.F. wishes to acknowledge the support of the Carl Reinhart Foundation.

APPENDIX A: COLOR FACTORS OF NON-ABELIAN CUT DIAGRAMS

Color factor of non-Abelian cut diagrams are calculated using the graphical rules in Fig. 3. Some explicit examples are shown in Figs. 6–9. In what follows, we shall discuss some of the general properties in the leading-log approximation.

Figure 3(c) can be used to get rid of cuts on the complementary cut diagrams. As a result, diagrams with $m-1$ uncut propagators along the upper tree have at most m gluon lines attached to it. We say ''at most,'' because relations 3(b), 3(d), and 3(e) can sometimes be used to get rid of more lines.

Since cuts are made on the upper tree, the number of gluons n attached to the lower tree is often larger than the number m attached to the upper tree. However, by using Fig. 3 again to manipulate the lines attached to the lower tree, at least in all cases encountered in Sec. IV, one can reduce the lines attached to the lower tree to be m. Hence, complementary cut diagrams with $m-1$ uncut propagators along the upper tree contribute color factors with m-Reggeized gluons, or less. It was then argued in Sec. III of the text that we need not keep those with less than m Reggeons in the leading-log approximation.

It is conceivable, for very complicated diagrams, that we cannot reduce n to m with the rules of Fig. 3 alone. The resulting color factor has $n\neq m$, so it cannot possibly contribute if Fig. 1 is the final result. For that reason we shall define the leading-log approximation to exclude all such color factors that cannot be reduced to $n=m$.

Using Figs. 3(b) and 3(c) again, the positions of gluon lines attached to the upper or the lower tree can be reversed; their difference being a diagram with one less gluon line attached to the upper or lower tree and, hence, can be ignored in the leading-log approximation. This is why primitive color factors can cross one another in any way along the upper and the lower trees, yet giving exactly the same result in the leading-log approximation.

Finally, we want to prove that any color factor with an s-line climbing onto the underside of a horizontal line, such

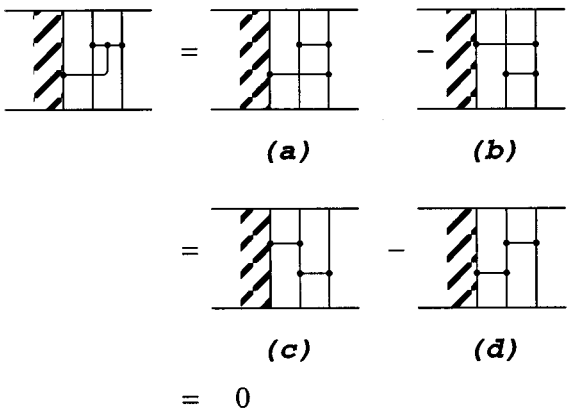

FIG. 11. Proof that an SCC diagram cannot yield a nonvanishing connected diagram that is not primitive. Within the leading-log approximation, Fig. 11(c)=Fig. 11(b) and Fig. 11(d)=Fig. 11(a).

as those found in Figs. 8 and 9, would be zero. The proof is shown in Fig. 11, where the shaded area can contain a very complicated structure. Use Figs. 3(b) and 3(c) (for four-gluon lines) to move the point joining the bottom of the horizontal line to the right, one gets Figs. 11(a) and 11(b). Moving that point to the left, one gets Figs. 11(c) and 11(d). Within the leading-log approximation, we can pull the middle vertical line of Fig. 11(c) to the extreme right to get Fig. 11(b), hence Fig. 11(b)=Fig. 11(c). Similarly, Fig. 11(a) =Fig. 11(d). Therefore, Fig. 11(a)−Fig. 11(b)=−[Fig. 11(a)−Fig. 11(b)]=0.

APPENDIX B: SATURATED LADDER DIAGRAMS

We want to show in this appendix that an SC diagram (see Sec. IV for notation) with two adjacent uncut propagators is unsaturated. By definition, a saturated diagram of $(2n)$th order and mRG exchange $(m-1$ cut lines) have a g and s dependence $g^{2m}(g^2\ln s)^{n-m}$. An unsaturated diagram is one with a slower s growth in comparison.

Reference [7] contains explicit calculations to $O(g^6)$. By examining Fig. 7 and Eq. (6.1) of that reference, it can be seen that this assertion is valid to $O(g^6)$. If one now follows the calculation of these examples with the method of Ref. [5] and Appendix B of Ref. [7], one can see that these calculations can easily be generalized to a multiloop situation as follows.

Consider an SC diagram with $n=l-1$ gluon lines. Let $q_i=(q_{i+},q_{i-},q_\perp)$ $(1\leqslant i\leqslant l)$ be the gluon momenta in the light-cone coordinates, and $q_{i-}\equiv x_i\sqrt{s}$.

We shall follow Ref. [5] by calculating the high energy behavior using residue calculus and flow diagrams to carry out the ''+'' integrations. For SC diagrams without adjacent uncut propagators, there is a unique flow path for each diagram, and the poles for the ''+'' integration can always be taken along the lower tree. The gluon propagators are then $\sim 1/q_{i\perp}^2$, and are considered to be of order 1. This leaves the uncut propagators along the upper tree to the ''−'' integration, each of which contributes to a factor of ln$s$ via ''−'' integration of the type $\int_{s^{-1}} dx_i/x_i$. Hence, such diagrams have their full share of ln$s$ factors and are saturated.

For diagrams with two adjacent uncut propagators, the flow path is never unique: the flow direction along the boundary of the two adjacent uncut loops cannot be determined. See Figs. 10.7 and 10.8 of Ref. [5] for concrete examples. As a result, at least one pole from the ''+'' integration must *not* come from the lower tree. Explicit calculation then shows that such diagrams are at least 1 ln$s$ power down from the saturated ones.

The origin of this reduction can be seen as follows. The ''+'' momentum is inversely proportional to the ''−'' momentum at the poles. Elsewhere, the ''+'' momenta are determined by momentum conservation. Now the ''−'' momentum flows predominantly along the lower tree, so if the pole is off it on a gluon line, the ''+'' momentum flowing through that line would be relatively large. By momentum conservation, there must be a return flow passing through part of the lower tree and another gluon line, and the Feynman propagators of these are large because of the large ''+'' flow through them. This brings about at least two small factors x_i overcompensating the large factor $1/x_i$ from the residue of the pole. This costs at least a ln$s$ factor to be lost from the ''−'' integration. Hence, the diagram is unsaturated.

[1] F. E. Low, Phys. Rev. D **12**, 163 (1975); S. Nussinov, Phys. Rev. Lett. **34**, 1286 (1975).

[2] L. N. Lipatov, Yad. Fiz. **23**, 642 (1976) [Sov. J. Nucl. Phys. **23**, 338 (1976)]; Ya. Ya. Balitskii and L. N. Lipatov, *ibid.* **28**, 1597 (1978) [*ibid.* **28**, 822 (1978)]; E. A. Kuraev, L. N. Lipatov, and V. S. Fadin, Zh. Eksp. Teor. Fiz. **71**, 840 (1976) [Sov. Phys. JETP **44**, 443 (1976)]; *ibid.* **72**, 377 (1977) [*ibid.* **45**, 199 (1977)]; V. Del Duca, Report No. hep-ph/9503226 (unpublished).

[3] C. Y. Lo and H. Cheng, Phys. Rev. D **13**, 1131 (1976); **15**, 2959 (1977); H. Cheng, J. A. Dickinson, and K. Olaussen, *ibid.* **23**, 534 (1980).

[4] V. S. Fadin, R. Fiore, and M. I. Kotsky, Phys. Lett. B **387**, 593 (1996).

[5] H. Cheng and T. T. Wu, *Expanding Protons: Scattering at High Energies* (MIT, Cambridge, MA, 1987).

[6] N. T. Nieh and Y. P. Yao, Phys. Rev. Lett. **32**, 1074 (1974); Phys. Rev. D **13**, 1082 (1976); B. McCoy and T. T. Wu, Phys. Rev. Lett. **35**, 604 (1975); Phys. Rev. D **12**, 3257 (1975); **13**, 1076 (1976); L. Tyburski, *ibid.* **13**, 1107 (1976); L. L. Frankfurt and V. E. Sherman, Yad. Fiz. **23**, 1099 (1976) [Sov. J. Nucl. Phys. **23**, 581 (1976)]; A. L. Mason, Nucl. Phys. **B117**, 493 (1976).

[7] Y. J. Feng, O. Hamidi-Ravari, and C. S. Lam, Phys. Rev. D **54**, 3114 (1996).

[8] C. S. Lam and K. F. Liu, Nucl. Phys. **B683**, 514 (1996).

[9] H. Cheng and T. T. Wu, Phys. Rev. **186**, 1611 (1969); M. Levy and J. Sucher, *ibid.* **186**, 1656 (1969).